

Numerical simulation of borehole Stoneley wave reflection by a fracture based on variable grid spacings method --Manuscript Draft--

Manuscript Number:	AGPH-D-18-00739
Full Title:	Numerical simulation of borehole Stoneley wave reflection by a fracture based on variable grid spacings method
Article Type:	Research Article
Abstract:	<p>In this paper, the finite difference method is used to model the Stoneley wave reflection by a horizontal fracture in a borehole. The fracture shape is described by some finite difference grids. Therefore, the fracture aperture can be varied in the radial direction, thus extending previous researches on the assumption that the fracture aperture is constant throughout the fracture. Finite difference grids can also be used to described a fracture which extends a finite distance in the radial direction. In addition, the finite difference algorithm can hold the problem of inhomogeneous formation. Therefore, it allows the elasticity of formation varies in the model. Very fine grids are needed to describe the small fracture aperture, that the variable grid spacings finite difference method is employed to improve computational efficiency. The Stoneley wave propagation is simulated by the variable grids spacing finite difference method in several models with variable fracture aperture with finite extension fracture, as well as models with heterogeneous formation.</p> <p>The variable grid spacings finite difference method is validated by a comparison with results of real axis integration method and the analytical method. By simulating and investigating effects of the variation of fracture aperture, the fracture of finite extent and inhomogeneity of formation on the Stoneley wave reflection, we get some conclusions. Although the fracture aperture changes along the fracture extension direction, the reflection coefficient of Stoneley wave is mainly controlled by the fracture aperture near the borehole. The Stoneley wave in the fracture is reflected by the tip of finite extension fracture and back into the borehole, which results in some notches in the reflection coefficient curve. If the Stoneley wave propagates from the formation with small elastic modulus to the formation with large elastic modulus, the reflection coefficient of Stoneley wave will increase. And if Stoneley wave propagates from the formation with large elastic modulus to the formation with small elastic modulus, the reflection coefficient of Stoneley wave will decrease. These results provide some basis for the use of Stoneley wave to detect the fracture properties in formation.</p>

Numerical simulation of borehole Stoneley wave reflection by a fracture based on variable grid spacings method

Ou Weiming, Wang Zhuwen*, Ning Qinqin, Xu Fanghui and Yu Yang

College of Geo-Exploration Science and Technology, Jilin University, Changchun 130021, China

ABSTRACT

In this paper, the finite difference method is used to model the Stoneley wave reflection by a horizontal fracture in a borehole. The fracture shape is described by some finite difference grids. Therefore, the fracture aperture can be varied in the radial direction, thus extending previous researches on the assumption that the fracture aperture is constant throughout the fracture. Finite difference grids can also be used to describe a fracture which extends a finite distance in the radial direction. In addition, the finite difference algorithm can hold the problem of inhomogeneous formation. Therefore, it allows the elasticity of formation varies in the model. Very fine grids are needed to describe the small fracture aperture, that the variable grid spacings finite difference method is employed to improve computational efficiency. The Stoneley wave propagation is simulated by the variable grids spacing finite difference method in several models with variable fracture aperture with finite extension fracture, as well as models with heterogeneous formation.

The variable grid spacings finite difference method is validated by a comparison with results of real axis integration method and the analytical method. By simulating and investigating effects of the variation of fracture aperture, the fracture of finite extent and inhomogeneity of formation on the Stoneley wave reflection, we get some conclusions. Although the fracture aperture changes along the fracture extension direction, the reflection coefficient of Stoneley wave is mainly controlled by the fracture aperture near the borehole. The Stoneley wave in the fracture is reflected by the tip of finite extension fracture and back into the borehole, which results in some notches in the reflection coefficient curve. If the Stoneley wave propagates from the formation with small elastic modulus to the formation with large elastic modulus, the reflection coefficient of Stoneley wave will increase. And if Stoneley wave propagates from the formation with large elastic modulus to the formation with small elastic modulus, the reflection coefficient of Stoneley wave will decrease. These results provide some basis for the use of Stoneley wave to detect the fracture properties in formation.

Key words: fracture; Stoneley wave; variable grid spacings; borehole

INTRODUCTION

Fracture is not only the channel of fluid storage and seepage, but also controls the distribution of oil and gas reservoirs. Therefore, understanding the characteristics of fractures in formation is favorable for oil extraction, migration and monitoring. In the array acoustic logging, the existence of fractures will change the waveform of acoustic wave. It is of great significance to grasp the influence of the different shapes of fractures for the array acoustic logging waveform by numerical simulation.

When a Stoneley wave in the borehole encounters a permeable fracture, it will reflect and attenuate. The fracture aperture can be calculated according to the reflection coefficient of Stoneley

* E-mail: wangzw@jlu.edu.cn

1 wave (Hornby et al. 1989 and 1992). A fracture is ~~regard~~ as a thin parallel planar layer ~~commonly~~.
2 Many analytical methods are used to model the propagation of Stoneley wave in a fluid filled borehole
3 intersected by a fluid filled fracture. In this respect, Hornby et al. (1989) presumed formation to be
4 rigid and calculated the relationship between reflection coefficient of Stoneley wave and fracture
5 aperture. Spring and Dudley (1992) considered the higher-order modes, and used the velocity potential
6 integral equation to ~~deduce~~ the Stoneley wave propagation in a borehole with fractures. Tang and
7 Cheng (1993) regarded a fracture as a permeable zone and developed a theory for the Stoneley wave
8 interaction with a borehole fracture. Tang (1990) considered the effect of elasticity of the fracture wall,
9 and in this theory, transmission coefficient was smaller than that in rigid formation theory. Kostek et al.
10 (1998b) considered the effects of some models including the combination of fractures and washouts,
11 elastic formation and multiple fractures on the reflection coefficient of Stoneley waves. Ionov (2007)
12 investigated ~~Stoneley wave excitation~~ in a borehole intersected by a horizontal fracture, by P-wave
13 propagating in the surrounding formation. Bakku et al. (2011 and 2013) considered the effect of
14 fracture compliance on the propagation of the Stoneley wave and proposed that measuring the
15 transmission coefficient can help constrain fracture compliance and aperture. The reflection coefficient
16 of Stoneley wave can be easily calculated by analytical methods, so analytical methods can be applied
17 to inversion of fracture aperture efficiently. However, these analytical methods can't deal with the
18 inhomogeneity of formation. Kostek et al. (1998a) developed a new finite difference (FD) scheme to
19 ~~obviate~~ the necessity for grids to describe fractures, and ~~for saving~~ computational time and memory.
20 And elastic properties of the formation can ~~be varied~~ radially and axially in this FD method. ~~However,~~
21 fracture aperture is assumed to be constant throughout the fracture ~~in all these studies mentioned above~~.

22
23 The fracture aperture of a naturally occurring fracture varies along the direction of the fracture
24 extension slowly (Brown et al. 1985 and 1986). The hydraulic fracture aperture near the borehole is
25 usually larger than that far from the borehole. The irregular shape of fracture can be described by some
26 FD grids. Stephen et al. (1985) had attempted to model the effects of horizontal fractures on acoustic
27 wave propagation by finite difference method, ~~since there is insufficient of this method to deal~~ with
28 discontinuous grids, they used coarse grid to model a fracture with an aperture of 8 cm. In fact, the
29 fracture aperture is less than 1 mm, ~~it~~ needs at least a few grid nodes to define the aperture of a thin
30 fracture. Therefore, very fine FD grids are ~~need~~ to describe the fracture shape. To model a thin fracture,
31 the FD method with constant grid needs very fine grid in the all computation region. This leads to
32 over-sampling of formations in space, which greatly increases the calculation time.

33
34 The variable grid steps (VGS) FD method can be used to simulate such a thin layer model (Moczo
35 1989; Aoi and Fujiwara 1999; Falk et al. 1996; Pitarka 1999). In the VGS FD method, grid spacings are
36 smoothly varied from elastic formation to the vicinity of the fracture, thus reducing the amount of data
37 and computing time. The VGS FD method can be used to simulate the scattering of waves which is
38 generated by fractures (Groenenboom and Falk 2000; Wu et al. 2005). Yan et al. (2015) modeled the
39 propagation of acoustic waves in borehole with tilted fractures within porous formation by VGS FD
40 method. In VGS FD method, the computational region is divided into several regions with different
41 grid steps, ~~we~~ use fine grid spacing in fracture region and its vicinity, and use coarse grid spacing in
42 formation region. Compared with the FD method with a constant grid spacing, the VGS FD method
43 costs much less computation time and memory. Therefore, we use the VGS FD method to simulate the
44 Stoneley wave propagation in the borehole inserted by a horizontal fracture. The main work of this
45 paper is to study effects of fracture with aperture variation, fracture of finite extent and inhomogeneous

formation on the reflection coefficient of Stoneley wave caused by the fracture.

In this paper, the VGS FD method is developed to simulate the Stoneley wave propagation in a borehole surrounded by a homogeneous elastic formation firstly. The simulated waveform is then compared with that obtained by the real axis integration (RAI) method proposed by Tsang and Rader (1979) to verify the validity of the VGS FD method. Later, the VGS FD method is used to simulate the Stoneley wave reflection in a borehole inserted by a flat fracture. The reflection coefficient of Stoneley wave obtained by the VGS FD method is also validated by a comparison with that calculated by the analytical method. Finally, the Stoneley wave reflection is simulated by the VGS FD method in several models with fracture aperture variation with fracture of finite extent, as well as models with heterogeneous formation, and effects of these models on the Stoneley wave reflection are investigated.

Model and Theory

The model of a borehole inserted by a horizontal fracture

Figure 1 is the configuration of a borehole intersected by a horizontal fracture on r - z plane. The fracture is sandwiched between two elastic formations. We assume that the model is axis-symmetric. The borehole and the fracture are full-filled with water. The speed of sound in water is v_f , $v_f = 1500$ m/s, and the water density ρ_f is 1000 kg/m^3 . The monopole source and receivers are located on the axis of the borehole. The fracture aperture can be variable, the extended distance of fracture can be finite or infinite. The radius of the borehole is a , and the fracture aperture is h . The extended distance of the fracture from borehole axis in radial direction is L . The solid circular and squares on the borehole axis represent the monopole source and receivers, respectively. The source is located below the fracture, and the distance from the fracture to the source is d , $d = 2$ m.

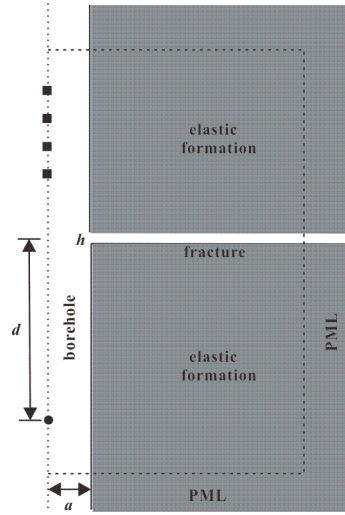


Fig. 1 The configuration of a borehole intersecting a horizontal fracture on r - z plane. The perfectly matched layer (PML) absorbing boundary is added to the boundary of the model.

First-order velocity-stress equations

Without considering the body force, the first-order velocity-stress equations for isotropic and elastic media are given by

$$\rho \frac{\partial \mathbf{v}}{\partial t} = \nabla \cdot \tau, \quad (1a)$$

and

$$\frac{\partial \tau}{\partial t} = \lambda (\nabla \cdot \mathbf{v}) \mathbf{I} + \mu (\nabla \mathbf{v} + \mathbf{v} \nabla), \quad (1b)$$

where \mathbf{v} stands for the particle velocity, τ is the stress tensor, λ and μ are the Lamé constants of media, \mathbf{I} is the identity tensor. The staggered grid FD method (Viriey 1986) is used to solve equation (1), and a second-order in space and in time approximation are applied. The borehole is cylindrical, so equation (1) is discretized in cylindrical coordinates. The formations surrounding the borehole are axis symmetric, so r - z plane scheme at any angle is used for simply equations. In r - z plane, the discrete equations of the point source can be expressed as

$$\begin{aligned} \sigma_i \rho_{(i-1/2, j+1/2)} (v_{r(i, j+1/2)}^{n+1/2} - v_{r(i, j+1/2)}^{n-1/2}) / \Delta t &= L_r \tau_{rr(i-1/2, j+1/2)}^n + L_z \tau_{rz(i, j)}^n \\ &+ (\sigma_i \tau_{rr(i-1/2, j+1/2)}^n - \sigma_i \tau_{\theta\theta(i-1/2, j+1/2)}^n) / r_i \end{aligned} \quad (1)$$

$$\begin{aligned} \sigma_j \rho_{(i+1/2, j-1/2)} (v_{z(i+1/2, j)}^{n+1/2} - v_{z(i+1/2, j)}^{n-1/2}) / \Delta t &= L_z \tau_{zz(i+1/2, j-1/2)}^n \\ &+ L_r \tau_{rz(i, j)}^n + \sigma_j \tau_{rz(i, j)}^n / r_{i+1/2} \end{aligned} \quad (2)$$

$$\begin{aligned} (\tau_{rr(i+1/2, j+1/2)}^{n+1} - \tau_{rr(i+1/2, j+1/2)}^n) / \Delta t &= (\lambda_{(i+1/2, j+1/2)} + 2\mu_{(i+1/2, j+1/2)}) L_r v_{r(i, j+1/2)}^{n+1/2} \\ &+ \lambda_{(i+1/2, j+1/2)} (L_z v_{z(i+1/2, j)}^{n+1/2} + \sigma_i v_{r(i, j+1/2)}^{n+1/2}) / r_{i+1/2} \end{aligned} \quad (3)$$

$$\begin{aligned} (\tau_{zz(i+1/2, j+1/2)}^{n+1} - \tau_{zz(i+1/2, j+1/2)}^n) / \Delta t &= (\lambda_{(i+1/2, j+1/2)} + 2\mu_{(i+1/2, j+1/2)}) L_z v_{z(i+1/2, j)}^{n+1/2} \\ &+ \lambda_{(i+1/2, j+1/2)} (L_r v_{r(i, j+1/2)}^{n+1/2} + \sigma_i v_{r(i, j+1/2)}^{n+1/2}) / r_{i+1/2} \end{aligned} \quad (4)$$

$$(\tau_{rz(i, j)}^{n+1} - \tau_{rz(i, j)}^n) / \Delta t = \mu_{(i-1/2, j-1/2)}^H (L_z v_{r(i, j-1/2)}^{n+1/2} + L_r v_{z(i-1/2, j)}^{n+1/2}) \quad (5)$$

$$\begin{aligned} (\tau_{\theta\theta(i+1/2, j+1/2)}^{n+1} - \tau_{\theta\theta(i+1/2, j+1/2)}^n) / \Delta t &= \lambda_{(i+1/2, j+1/2)} (L_r v_{r(i, j+1/2)}^{n+1/2} + L_z v_{z(i+1/2, j)}^{n+1/2}) \\ &+ (\lambda_{(i+1/2, j+1/2)} + 2\mu_{(i+1/2, j+1/2)}) \sigma_i v_{r(i, j+1/2)}^{n+1/2} / r_{i+1/2} \end{aligned} \quad (6)$$

In the equations mentioned above, the superscript n represents the time discrete index, the subscripts i and j refer to spatial position index of nodes in r and z directions respectively, Δt is the time sampling step, L_r and L_z refer to space difference operator in r and z directions respectively. The forward arithmetic averaging operators σ_i and σ_j are defined as $\sigma_i f_i = (f_i + f_{i+1})$ and $\sigma_j f_j = (f_j + f_{j+1})$.

The harmonic mean $\mu_{(i-1/2, j-1/2)}^H$ are defined as

$$\mu_{(i-1/2, j-1/2)}^H = 4 / (1 / \mu_{(i+1/2, j+1/2)} + 1 / \mu_{(i+1/2, j-1/2)} + 1 / \mu_{(i-1/2, j+1/2)} + 1 / \mu_{(i-1/2, j-1/2)}) \quad (8)$$

And at the interface "liquid-solid", $\mu_{(i-1/2, j-1/2)}^H$ is set to 0.

To reduce the numerical dispersion, the grid spacing needs to satisfy the following inequality:

$$\Delta_{max} \leq v_{min}/10f_{max}, \quad (4)$$

where Δ_{max} is the max grid spacing, v_{min} is the minimum velocity of the model and f_{max} is the maximum frequency of the source. The stability condition of the second order FD method is

$$v_{max}\Delta t[1/\Delta r^2 + 1/\Delta z^2]^{1/2} < 1, \quad (5)$$

where v_{max} is the maximum velocity of the model.

Variable Grids Steps (VGS) Finite Difference Method

The scheme of VGS FD method


For the FD method with const grid spacing, grid spacing is determined by the smallest length scale to be modeled and the smallest wavelength of the model. To model the formation with a very thin fracture, the general FD method requires a grid spacing of several tens of microns to describe a few meters long model. This requires a large amount of data to be calculated, thus increasing a large amount of computation time. Therefore, we choose the VGS FD method developed by Aoi and Fujiwara (1999) to improve computational efficiency. Because the second-order FD method is used in this paper, it is not necessary to interpolate the values of the overlapping regions of coarse and fine grids. 

Figure 2 shows the smooth change mechanism of the grid spacing from the area away from the fracture to the vicinity of fracture. From the area far from the fracture to the vicinity of the fracture, the grid steps in z -direction are as follows: $\Delta z(1)$, $\Delta z(2)$, $\Delta z(3)$, $\Delta z(4)$ and $\Delta z(5)$. The fracture extends along the r -direction, and the coarse grid is enough to describe the fracture length. According to inequality (4), the grid spacing Δr is taken to be constant with a value of 1 cm in the r -direction. Similarly, the grid spacing $\Delta z(1)$ in the area away from the fracture is 1 cm. The horizontal fracture aperture h is 80 μm , five fine grids are used to describe the fracture aperture, thus the grid spacing $\Delta z(3)$ is 16 μm . Because of the properties of staggered grids, the jump ratio of grid spacing is an odd integer. For the fracture aperture in fig. 3, the jump ratio chosen is 5. Therefore, $\Delta z(2)$, $\Delta z(3)$ and $\Delta z(4)$ are 2000 μm , 400 μm and 80 μm , respectively. The whole model is divided into different computation regions depending on different grid spacings. The boundaries of adjacent computational regions are overlapped. Considering the stability condition of the FD method and the efficiency of the computation program, the fine grid spacing is adjusted according to the size of fracture aperture. By this way, the grid spacing is varied smoothly from 1 cm to 16 μm .

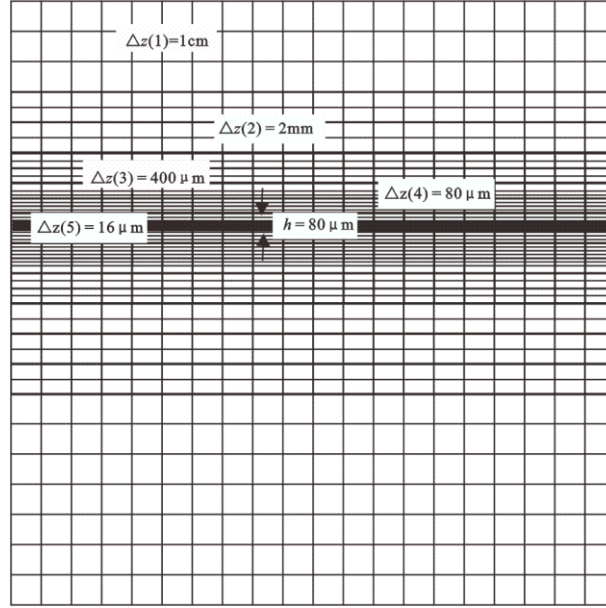


Fig. 2 The variable grids FD scheme in the formation with a fracture. The black thick lines represent the horizontal fracture. The axial grid number of computation region whose grid spacing Δz is $\Delta z(2)$, $\Delta z(3)$, $\Delta z(4)$ or $\Delta z(5)$ is 22.

The time step Δt should be chosen from the inequality (5) according to the minimum grid step. To simulate the propagation acoustic wave, the detailed steps of employing the VGS FD scheme are as follows:

1. The monopole source is added to the normal stress component. Formula (2e) and (2f) are used to calculate the velocity component value of each computational region at the time $t = 1/2\Delta t$.
2. The velocity components of each boundary between the adjacent computational regions are transferred to each other.
3. Formula (2a), (2b), (2c) and (2d) are used to calculate the stress values of each computational region at the time $t = \Delta t$.
4. The stress component values of each boundary between the adjacent computational regions are also transferred to each other.

By repeating the above steps, we can calculate the wavefield at each time in the model, and obtain waveforms of acoustic wave propagation.

Verifying the Results of the VGS FD Method

Waves in homogeneous formation

To validate the FD method, we used VGS FD method to simulate the propagation of acoustic waves in the borehole surrounded by a homogeneous elastic formation without a fracture. Parameters of the elastic formation are Formation I listed in Table 1. The axial and radial lengths of the model are 6.4 m and 1.28 m, respectively. The scheme of the VGS is shown in fig. 2. The selected time step Δt is 525 μ s. The non-splitting perfectly matched layer (PML) absorbing boundary (Wang and Tang 2003) is added in the model boundary, as shown in fig. 1. The GPU-based parallel technology is used to improve the computational efficiency. The graphics card used is GeForce GTX 1060, and this computation program costs about 3.2 hours.

Then we verify this FD method with the results of the RAI method. The comparison of the

waveforms between these two methods is shown in Fig. 3. The distance from the source to the first receiver is 1.0 m, and the interval between receivers is 0.2 m. The source is the Ricker wave and its center frequency is 10 kHz. The waveforms of these two methods are matched excellently, which shows that the FD method is effective. The small differences in amplitude are caused by FD grid dispersion and the discrete Fourier transforms.

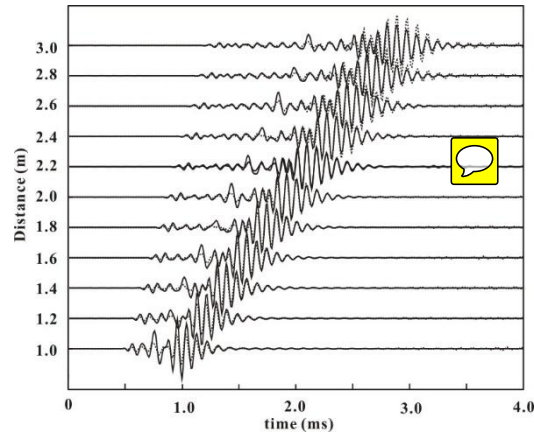


Fig. 3 The comparison of the waveforms between FD method (dashed curves) and RAI method (solid curves) in the homogeneous formation. The distance from the source to the first receiver is 1.0 m, and the interval between receivers is 0.2 m, the center frequency is 10 kHz.

Table 1. Physical parameters of the elastic formation.

Formation	v_p m/s	v_s m/s	ρ kg/m ³
Formation 1	4000	3000	2800
Formation 2	4000	2700	2650
Formation 3	5000	3000	2700

Numerical Simulation Results

Wavefields and waveforms of the Stoneley wave propagating in a borehole inserted by a horizontal fracture

We used the VGS FD method to simulate the propagation of Stoneley waves in the borehole inserted by an infinitely extended fracture. The constant aperture of fracture is 1 mm. Elastic formations on both sides of the fracture are Formation 1 listed in Table 1. The center frequency of the source is 1.5 kHz. Under such a low frequency condition, compressional waves and shear waves can't be excited, and there are only Stoneley waves in the borehole. The wavefields of the Stoneley wave propagation in the borehole intersected by a fracture are shown in Fig. 4. At the time of 2 ms, the energy of the waves is mainly concentrated in the borehole. At the time of 2.75 ms, we note that some waves are excited in the fracture. At the time of 4 ms, we can see that some waves propagate along the fracture, and some waves are reflected.

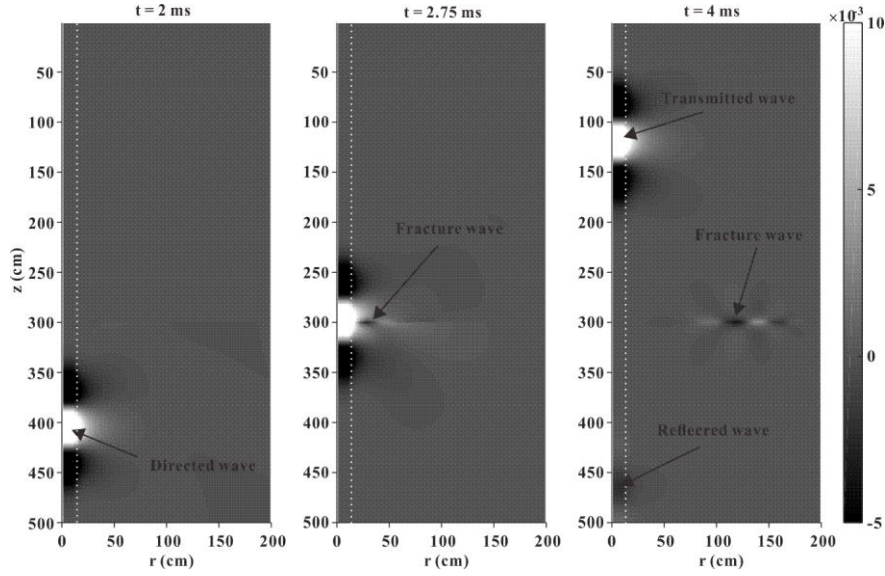


Fig. 4 The wavefields of the Stoneley wave propagation in the borehole intersected by a fracture. The fracture is located at a position of $z = 300$ cm, the point source is located at a $z = 500$ cm and $r = 0$ cm, the dashed line is the interface between borehole and formation.

The waveforms of Stoneley wave corresponding to Fig. 4 are shown in Figure 5. The distance from the source to the first receiver is 1.0 m, and the interval between receivers is 0.2 m. The fracture is 2.0 m above the source. It can be seen that the receivers under the fracture recorded obvious reflected waves.

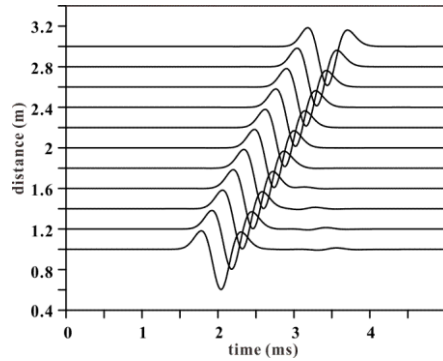


Fig. 5 The propagation of Stoneley wave in the borehole with a single fracture. The distance from the source to the first receiver is 1.0 m, and the interval between receivers is 0.2 m, the center frequency of the source is 1.5 kHz.

Comparison between the VGS method and analytical methods

The analytical formula used to calculate the reflection coefficient $r(\omega)$ of Stoneley wave is as follow (Kostek et al. 1998b):

$$r(\omega) = -\frac{ihk_r H_1^1(k_r a) / aH_0^1(k_r a)}{k_T + ihk_r H_1^1(k_r a) / aH_0^1(k_r a)}, \quad (12)$$

where k_T is the Stoneley wavenumber of the elastic formation, $k_T = \omega / v_T$. The velocity of Stoneley

1 wave is v_T , $v_T = 1/(1/v_f^2 + \rho_f / \rho v_s^2)^{1/2}$.

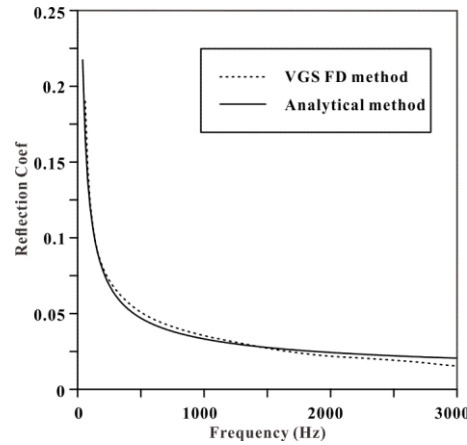
2
3 In the case of the borehole intersected by a fracture, the simulated Stoneley wave includes direct
4 wave and reflected wave, as shown in fig. 5. We also simulated Stoneley wave propagation in the
5 borehole without a fracture to obtain the direct waves. The direct waves are subtracted from the
6 simulated Stoneley waves to separate reflected waves .
7
8

9 To obtain the reflection coefficient in frequency domain, the Fourier transform is used to obtain
10 the frequency spectrum of direct and reflected waves. The reflection coefficient of Stoneley wave can
11 be calculated by
12

$$13 \quad r(\omega) = R(\omega) / D(\omega) , \quad (13)$$

14 where $R(\omega)$ is the frequency spectrum of reflected Stoneley wave, $D(\omega)$ refer to frequency spectrum of
15 direct Stoneley wave in homogeneous formation.
16

17 Figure 6 shows the magnitude of Stoneley wave reflection coefficients which are calculated from
18 the VGS FD method (dotted curves) and analytic models (solid curves). The two elastic formations on
19 both sides of the fracture are Formation 2 listed in Table 1. The fracture is an infinite and horizontal
20 parallel-plate, and the fracture aperture is 1mm. It can be seen that the reflection coefficient of the VGS
21 FD method is very close to that of the analytical method.
22
23
24



25
26
27
28
29
30
31
32
33
34
35
36
37
38
39
40
41 **Fig. 6** The comparison of the reflection coefficients by fracture between FD method (dashed
42 curves) and analytical method (solid curves).
43

44 **Effect of fracture with aperture variation**

45 The aperture of a nature fracture is not constant throughout the fracture. During drilling, the
46 aperture of some fracture openings is enlarged by the mechanical force. These lead to the variation of
47 the fracture aperture in the radial direction. We have designed two kinds of simple fracture models with
48 aperture variation, namely Fracture a and Fracture b, as shown in Figure 7. For Fracture a, the fracture
49 aperture near the borehole is h_1 , and the fracture aperture decreases gradually to h_2 from the location
50 where the distance to the borehole axis is l . For Fracture b, the variation of fracture aperture is just
51 opposite to that of Fracture a. We simulated reflected Stoneley waves caused by these two fractures.
52
53
54
55
56
57
58
59
60
61
62
63
64
65

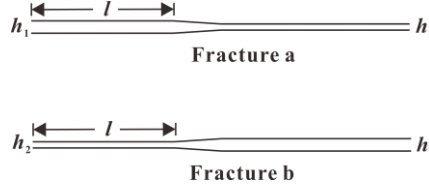


Fig. 7 Two fracture models with aperture variation.

Very fine FD grids are used to describe the fractures with aperture variation, as shown in Figure 8. The aperture of Fracture a varies from 0.82 mm to 0.24 mm, and the aperture of Fracture b varies from 0.24 mm to 0.82 mm, they correspond to Fig. 8a and Fig. 8b respectively. The distance l is 20 cm. Grid spacings Δz and Δr are 40.8 μm and 1cm respectively. Thus i_1 and i_2 are 21 and 28 respectively, $j_2 - j_1 = 20$ and $j_4 - j_3 = 6$. The two elastic formations on both sides of the fracture are Formation 2 listed in Table 1. To highlight the effect of fractures with varying apertures on the reflection coefficient of Stoneley wave, we also simulated two fractures with constant apertures, whose apertures were 0.82 mm and 0.24 mm respectively.

Figure 9 shows the reflection coefficient of Stoneley wave corresponding to Fracture a and Fracture b. Several notches appear in the reflection coefficient curve corresponding to fractures with varied aperture. This is because the variation of fracture aperture causes the reflection of Stoneley waves propagating along the fracture, and the reflected waves propagate back from the fracture to the borehole and superimpose with the waves in the borehole. Note that the reflection coefficient of Fracture a (dotted curve) is close to that of the fracture with 0.82 mm aperture (solid curve), while the reflection coefficient of Fracture b (dashed curve) is close to that of fracture with 0.24 mm aperture (dotted-dashed curve). This shows that the reflection coefficient of Stoneley wave is mainly controlled by the aperture of the fracture opening.

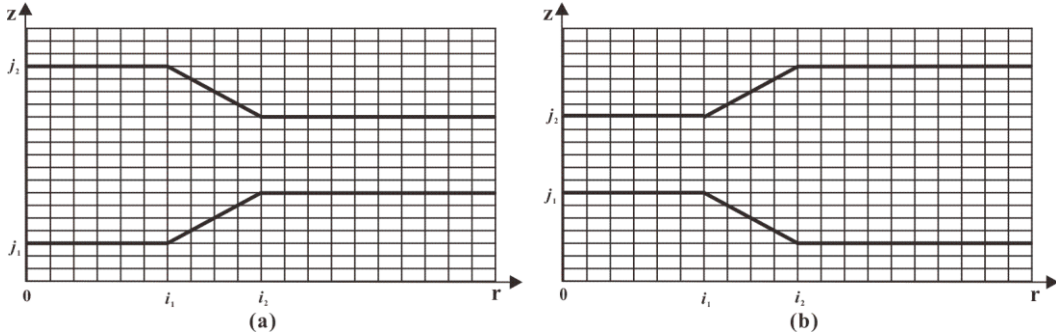


Fig. 8 Very fine FD grids are used to describe the fractures with aperture variation. Figure a and b represent Fracture a and Fracture b respectively.

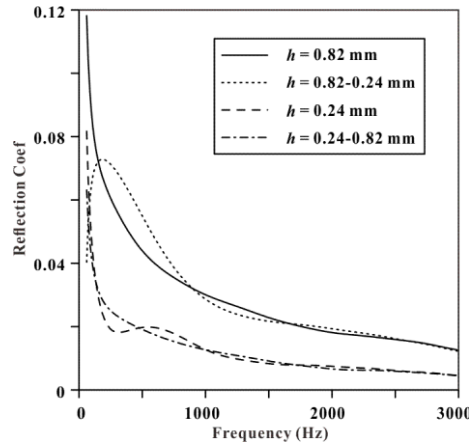


Fig. 9 Reflection coefficients of Stoneley wave caused by fractures with aperture variation. The solid curve and dotted-dashed curve represent reflection coefficient for a fracture with a constant aperture of 0.82 mm and 0.24 mm respectively. The dotted curve and dashed curve represent reflection coefficient for Fracture a and Fracture b respectively.

Effect of fracture of finite extent

Hornby et al. (1989) established a formula for calculating the reflection coefficient of Stoneley wave caused by a finitely extended fracture in a rigid formation. The reflection of Stoneley wave by a finitely extended fracture in elastic formation is simulated by using the VGS FD method. The fractures extend radially from the borehole axis to a finite distance L . The fracture aperture is 1 mm. Elastic formations on both sides of the fracture are Formation 2 listed in Table 1. Figure 10 shows the waveforms of the Stoneley wave propagation in the borehole with a finite extended fracture. In Fig. 10a and 10b, the extended distances of fractures are 0.3 m and 0.5 m respectively. It can be seen obviously that there are multiple sets of reflected Stoneley waves. The first group of reflected waves is caused by elastic differences between fracture openings and elastic formation. The other reflected waves are formed due to Stoneley waves propagating along the fracture extension direction are reflected back into the borehole by the tip of the fracture.

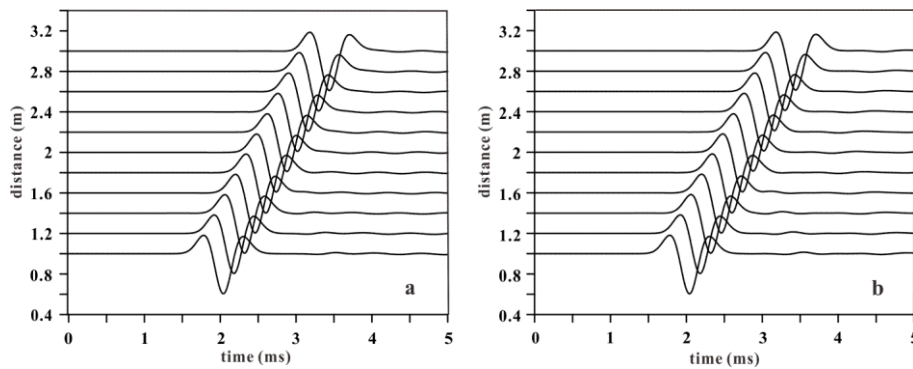


Fig. 10 Waveforms of the Stoneley wave propagation in the borehole with a finite extended fracture. In figure a and b, the extended distances of fractures are 0.3 m and 0.5 m respectively.

The reflection coefficient of the Stoneley wave is calculated by using the waveform in Fig. 10, as shown in Figure 11. Due to the superposition of multiple reflected Stoneley waves, a series of notches appear in reflection coefficient curves of Stoneley waves corresponding to the finitely extended

fractures, and reflection coefficients increase a lot at low frequencies. Reflection coefficients of finitely extended fractures are around that of the infinitely extended fracture. We calculate the reflection coefficient only by choosing the first reflected Stoneley wave of the fracture with an extended distance L of 0.5 m, as shown in Figure 12. The reflection coefficient calculated from the first reflected Stoneley wave of the fracture with an extended distance is very close to that of the infinitely extended fracture. It can be known that when the fracture extends far enough, the reflected Stoneley wave caused by the tip of the fracture can not be recorded due to the limitation of sampling time, and the reflection coefficient of finitely extended fracture is consistent with that of the infinitely extended fracture.

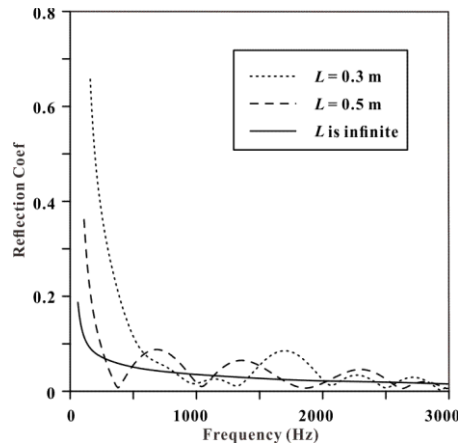


Fig. 11. Reflection coefficient of the Stoneley wave caused by the fracture of finite extent. The dotted curve, dashed curve and solid curve represent reflection coefficient by a fracture with a extended distance of 0.3m, 0.5m and infinite, respectively.

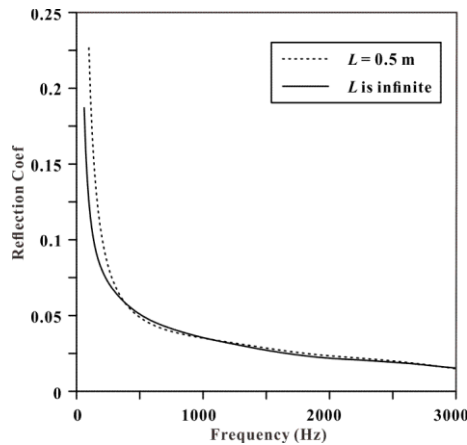


Fig. 12 Comparison between the reflection coefficient calculated from the first reflected Stoneley wave of the fracture with an extended distance (dotted curve) and that for the infinite fracture (solid curve).

Effect of inhomogeneous formation

In fact, the elasticity of formation often changes in radial and axial directions. We consider one of the inhomogeneous conditions, that is, elastic properties of two formations on both sides of the fracture are different. The borehole Stoneley wave number varies with formation elasticity, and the difference of Stoneley wave number will affect the reflection coefficient. In Fig. 1, we set up two different elastic formations on both sides of the fracture to explore the effect of elasticity difference on Stoneley wave reflection.

Figure 13 shows the reflection coefficient of Stoneley wave with axial change of formation elasticity. The fracture is infinitely extended, and the fracture aperture is 1 mm. Formation 2-3 represents Formation 2 above the fracture, while Formation 3 below the fracture. Formation 3-2 represents Formation 3 above the fracture and Formation 2 below the fracture. For homogeneous formation, the Stoneley wave reflection coefficient of formation 2 is larger than that of formation 3, which indicates that the reflection coefficient of Stoneley wave in formation with small elastic modulus is larger. The reflection coefficient of Formation 3-2 is larger than that of Formation 3, while the reflection coefficient of Formation 2-3 is less than that of Formation 2. It can be seen that if Stoneley wave propagates from the formation with small elastic modulus to the formation with large elastic modulus, the reflection coefficient of Stoneley wave will increase. And if Stoneley wave propagates from the formation with large elastic modulus to the formation with small elastic modulus, the reflection coefficient of Stoneley wave will decrease.

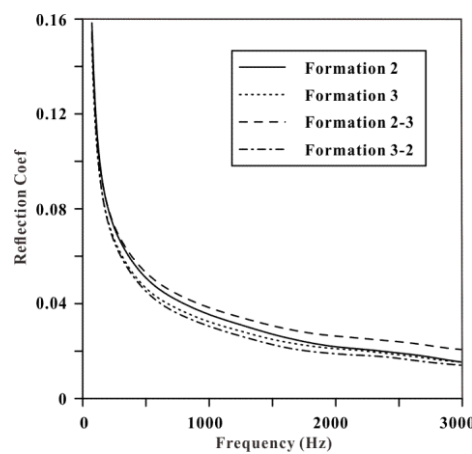


Fig. 13 Reflection coefficient of Stoneley wave with axial change of formation elasticity.

DISCUSSION AND CONCLUSIONS

In this paper, we employ the VGS FD method to simulate the Stoneley wave reflection by a horizontal fracture in a borehole. By using the VGS FD method, the effects of the variation of fracture aperture, the finite extent of fracture and the inhomogeneity of formation on Stoneley wave reflection coefficient are simulated. The VGS FD method is validated by comparing with the waveform of the RAI method and the reflection coefficient of the analytical method.

The reflection coefficient of Stoneley wave is affected by the variation of fracture aperture, the finite extension of fracture and the inhomogeneity of formation. Because of the change of fracture aperture, Stoneley waves in fractures are reflected back into the borehole, resulting in several notches in the reflection coefficient curve of Stoneley wave. Although the fracture aperture varies along the direction of the fracture extension, the reflection coefficient of Stoneley wave is mainly controlled by the fracture aperture near the borehole. Therefore, using the reflection coefficient of Stoneley wave to calculate the fracture aperture, we can only get the aperture near the borehole. The tip of a finitely extended fracture also causes reflection of the wave in the fracture, and then the reflected wave propagates back into the borehole, which leads to an increase in the reflection coefficient of Stoneley wave at low frequencies, and a series of notches appear in the reflection coefficient curve of Stoneley wave. Of course, the existence of these notches can be used to infer that fracture extends a finite distance, but it will increase the difficulty of calculating fracture aperture by the reflection coefficient.

For the fracture of finite extent, we can only choose the first reflected Stoneley wave to calculate the reflection coefficient. Because this reflection coefficient is very close to that of the infinitely extended fracture, we can use it to calculate the fracture aperture. The reflection coefficient of Stoneley wave increases, when Stoneley wave propagates from the formation with small elastic modulus to the formation with large elastic modulus. And when the reflection coefficient of Stoneley wave decreases, when Stoneley wave propagates from the formation with large elastic modulus to the formation with small elastic modulus. Therefore, the variation of elasticity of formation on both sides of the fracture should be taken into account when the reflection coefficient calculated by analytical method is used to invert the fracture aperture.

In this paper, fractures are assumed to be axis-symmetric. We realize that the natural fractures are rarely so symmetrical, and the computation procedure is very time-consuming. However, we convinced that the analyses for the effects of the variation of fracture aperture, the fracture of finite extent and the inhomogeneity of formation on Stoneley wave reflection coefficient will be helpful to the evaluation of fractures.

Acknowledgement

The work described in this paper is supported by the National Natural Science Foundation of China (No.41874135).

References

- Aoi S, Fujiwara H (1999) 3D finite-difference method using discontinuous grids. *Bulletin of the Seismological Society of America*, 89(4), 918-930.
- Bakku S K, Fehler M, Burns D (2011) Fracture characterization from tube waves in boreholes. *Transactions - Geothermal Resources Council*, 35, 1617-1622.
- Bakku S K, Fehler M, Burns D, (2013) Fracture compliance estimation using borehole tube waves. *Geophysics*, 78, D249–D260.
- Brown S R, Scholz C H (1985) Broad bandwidth study of the topography of natural rock surfaces. *Journal of Geophysical Research: Solid Earth*, 90(B14), 12575-12582.
- Brown S R, Kranz R L, Bonner B P (1986) Correlation between the surfaces of natural rock joints. *Geophysical Research Letters*, 13(13), 1430-1433.
- Falk J, Tessmer E, Gajewski D (1996) Tube wave modeling by the finite-difference method with varying grid spacing. *pure and applied geophysics*, 148(1-2), 77-93.
- Fan H, Smeulders D M J (2013) Shock-induced wave propagation over porous and fractured borehole zones: Theory and experiments. *Journal of the Acoustical Society of America*, 134, 4792.
- Groenenboom J, Falk J (2000) Scattering by hydraulic fractures: Finite-difference modeling and laboratory data. *Geophysics*, 65, 612-622.
- Hornby B E, Johnson D L, Winkler K W, Plumb, R A (1989) Fracture evaluation using reflected Stoneley-wave arrivals. *Geophysics*, 54, 1274-1288.
- Hornby B E, Luthi S M, Plumb R A (1992) Comparison of fracture apertures computed from electrical borehole scans and reflected Stoneley waves: an integrated interpretation. *The Log Analyst*, 33(01).
- Ionov A M (2007) Stoneley wave generation by an incident P-wave propagating in the surrounding formation across a horizontal fluid-filled fracture. *Geophysical Prospecting*, 55, 71–82.
- Kostek S, Johnson D L, Randall C J (1998a) The interaction of tube waves with borehole fractures. Part

I: Numerical models. *Geophysics*, 63, 800-808.

- 1 Kostek S, Johnson D L, Winkler K W, Hornby B E (1998b) The interaction of tube waves with
2 borehole fractures. Part II: Analytical models. *Geophysics*, 63, 809-815.
- 3 Kristek J, Moczo P, Galis M (2010) Stable discontinuous staggered grid in the finite-difference
4 modelling of seismic motion. *Geophysical Journal International*, 183, 1401–1407.
- 5 Moczo P (1989) Finite-difference technique for SH-wave in 2-D media using irregular
6 grids—Application to the seismic response problem: *Geophysics Journal International*, 99,
7 321–329.
- 8 Pitarka A (1999) 3D elastic finite-difference modeling of seismic motion using staggered grids with
9 nonuniform spacing. *Bulletin of the Seismic Society of America*, **89**, 54–68.
- 10 Spring C T, Dudley D G (1992) Acoustic wave propagation in a cylindrical borehole with fractures.
11 *Journal of the Acoustical Society of America*, 91, 658-669.
- 12 Stephen R A, Cardo-Casas F, Cheng C H (1985) Finite-difference synthetic acoustic logs. *Geophysics*,
13 50, 1588-1609.
- 14 Tsang L, Rader D (1979) Numerical evaluation of the transient acoustic waveform due to a point
15 source in a fluid-filled borehole. *Geophysics*, 44, 1706-1720.
- 16 Tang X M, Cheng C H (1989) A dynamic model for fluid flow in open borehole fractures. *Journal of*
17 *Geophysical Research*, 94, 7567-7576.
- 18 Tang X M, (1990) Acoustic logging in fractured and porous formations. ScD. thesis, Massachusetts
19 Institute of Technology.
- 20 Tang X M and Cheng C H (1993) Borehole Stoneley wave propagation across permeable structures.
21 *Geophysical Prospecting*, 41, 165–187.
- 22 Virieux J, (1986) P-SV wave propagation in heterogeneous media: Velocity-stress finite-difference
23 method. *Geophysics*, 51, 889-901.
- 24 Wang T, Tang X (2003) Finite-difference modeling of elastic wave propagation: a nonsplitting perfectly
25 matched layer approach. *Geophysics*, 68(5), 1749-1755.
- 26 Wu C L, Harris J M, Nihei K T, Nakagawa S, (2005) Two-dimensional finite-difference seismic
27 modeling of an open fluid-filled fracture: comparison of thin-layer and linear-slip models.
28 *Geophysics*, 70, T57–T62.
- 29 Yan S G, Xie F L, Gong D, Zhang C G, Zhang B X (2015) Borehole acoustic fields in porous
30 formation with thin fracture. *Chinese Journal of Geophysics*, 58, 307-317.
- 31
32
33
34
35
36
37
38
39
40
41
42
43
44
45
46
47
48
49
50
51
52
53
54
55
56
57
58
59
60
61
62
63
64
65